ADVANCED MATERIALS
www.advmat.de

Electro-Optic Modulation in Hybrid Metal Halide Perovskites

*Yuan Gao, Grant Walters, Ying Qin, Bin Chen, Yimeng Min, Ali Seifitokaldani, Bin Sun, Petar Todorovic, Makhsud I. Saidaminov, Alan Lough, Sefaattin Tongay, Sjoerd Hoogland, and Edward H. Sargent**

Rapid and efficient conversion of electrical signals to optical signals is needed in telecommunications and data network interconnection. The linear electro-optic (EO) effect in noncentrosymmetric materials offers a pathway to such conversion. Conventional inorganic EO materials make on-chip integration challenging, while organic nonlinear molecules suffer from thermodynamic molecular disordering that decreases the EO coefficient of the material. It has been posited that hybrid metal halide perovskites could potentially combine the advantages of inorganic materials (stable crystal orientation) with those of organic materials (solution processing). Here, layered metal halide perovskites are reported and investigated for in-plane birefringence and linear electro-optic response. Phenylmethylammonium lead chloride (PMA_2PbCl_4) crystals are grown that exhibit a noncentrosymmetric space group. Birefringence measurements and Raman spectroscopy confirm optical and structural anisotropy in the material. By applying an electric field on the crystal surface, the linear EO effect in PMA_2PbCl_4 is reported and its EO coefficient is determined to be 1.40 pm V^{-1}. This is the first demonstration of this effect in hybrid metal halide perovskites, materials that feature both highly ordered crystalline structures and solution processability. The in-plane birefringence and electro-optic response reveal that layered perovskite crystals could be further explored for potential applications in polarizing optics and EO modulation.

Optical anisotropy enables both linear and nonlinear optical properties, enabling applications such as polarizing optics, frequency upconversion, and electro-optic (EO) modulation. EO modulation relies on optical anisotropy and the changes to it that occur under electric fields. Optical anisotropy originates from a lack of symmetry in the material's structure: when a material lacks inversion symmetry, second-order nonlinear optical effects can occur. The linear EO effect, or Pockels effect, is of use in optical modulation for network interconnection and telecommunications.

Silicon photonics offers the possibility of condensing optical interconnects to intra-/interchip length scales. However, silicon-based EO modulators that exploit the plasma dispersion effect suffer from significant energy losses incurred in changing the carrier density; and they also require large device footprints, in light of a weak index change, that stand in the way of high-speed operation.[1]

The integration of high-performance nonlinear optical materials within photonic waveguides is therefore desired. The inorganic nonlinear crystals such as lithium niobate (LNO) and barium titanate (BTO) possess high phase transition temperatures (above 120 °C)[2,3] and large coercive field strengths (greater than 10^5 V m^{-1});[2] however, the integration of inorganic nonlinear crystals relies on costly and complicated bonding or deposition processes (heterogeneous integration).[4,5] Organic nonlinear optical molecules can be solution processed, and therefore offer convenient integration with on-chip photonic structures.[6–8] However, such organic molecules, which (individually) have impressively high EO coefficients, lose performance when they depole in light of thermodynamic instabilities in ordered films of organic molecules.[9,10]

The past decade has seen the rapid development of metal halide perovskite optoelectronics, including solar cells, light emitting diodes, lasers, and detectors. These materials are highly crystalline and can be solution processed, enabling integration with photonic structures. The most widely studied metal halide perovskites, which features the chemical structure $APbX_3$

Dr. Y. Gao, Dr. G. Walters, Dr. B. Chen, Y. Min, Dr. A. Seifitokaldani, Dr. B. Sun, P. Todorovic, Dr. M. I. Saidaminov, Dr. S. Hoogland, Prof. E. H. Sargent
Department of Electrical and Computer Engineering
University of Toronto
10 King's College Road, Toronto, Ontario M5S 3G4, Canada
E-mail: ted.sargent@utoronto.ca
Y. Qin, Prof. S. Tongay
School for Engineering of Matter
Transport and Energy
Arizona State University
Tempe, AZ 85287, USA
Dr. A. Lough
Department of Chemistry
University of Toronto
80 St. George Street, Toronto, Ontario M5S 3H6, Canada
The ORCID identification number(s) for the author(s) of this article can be found under https://doi.org/10.1002/adma.201808336.

DOI: 10.1002/adma.201808336

(A = $CH_3NH_3^+$, $^+HC(NH_2)$, Cs^+, and X = Cl, Br, I), have been studied for optical and electronic anisotropies.[11,12] Despite density functional theory (DFT) predictions showing high polarizations (14.03[13] or 38[14] μC cm^{-2} for $CH_3NH_3PbI_3$) and noncentrosymmetric crystalline structures,[13] only small polarizations (a few nC cm^{-2}) have been measured experimentally.[15] This small polarization is likely due to dynamic rotation and antiparallel alignment of the molecular cations.[15] The absence of global structural noncentrosymmetry has then lead to observations of only very weak second-order nonlinear optical effects: for example, second harmonic generation (SHG) was seen from $CH_3NH_3PbI_3$ to be less than 5% of that of quartz.[16] Third-order optical nonlinearities, which do not require noncentrosymmetry, such as the Kerr effect[17,18] and two-photon absorption,[19] have been well studied in hybrid metal halide perovskites. Many layered metal chalcogenide perovskites possess noncentrosymmetric structures;[20,21] however, they are usually prepared via solid reaction instead of via solution processing. In hybrid perovskites with a ferroelectric phase, SHG attests to the polarity of the crystals.[22–24] Other second-order nonlinear optical effects, such as the linear EO effect, have yet to be studied.

Reducing the dimensionality of the bulk perovskite to layered structures through the introduction of bulky ammonium-terminated spacer cations brings additional compelling properties. The 2D network of corner-sharing octahedra also acts as a scaffold that anchors and has the potential to align the long aliphatic- or aromatic-ammonium-terminated cations. The collective alignment of the bulky cations can introduce crystalline noncentrosymmetry and induce spontaneous polarization in the 2D perovskite, thereby allowing for observations of ferroelectricity and piezoelectricity.[22,25–27] Moreover, the 2D perovskites exhibit improved stability against moisture and heat compared to their 3D counterparts.[28] Due to the quantum confinement effect, the bandgap of the 2D perovskite is increased. As a result, the perovskite is transparent over a broader spectral range, permitting a wider window for the modulation wavelength.

Here we investigate a layered hybrid metal halide perovskite, phenylmethylammonium lead chloride (PMA_2PbCl_4), which belongs to a noncentrosymmetric space group and has an inherent polarization. The phase transition temperature of PMA_2PbCl_4 crystals is 165 °C,[22] higher than that of the inorganic nonlinear optical crystals BTO (123 °C)[2] and also above the typical glass-transition temperatures of organic nonlinear optical molecules.[10] Therefore, the linear EO effect from PMA_2PbCl_4 crystals is thermally stable, encouraging on-chip integration. Motivated by the noncentrosymmetric structure and high phase transition temperature, we studied the linear and nonlinear optical properties of PMA_2PbCl_4. We employed angle-resolved Raman spectroscopy and the measurement of the in-plane birefringence of PMA_2PbCl_4 to confirm its structural anisotropy. We present the first account of linear electro-optic modulation using a hybrid metal halide perovskite.

In order for a material to exhibit second-order nonlinear optical properties ($P \propto E^2$), a lack of inversion symmetry is required. This then leads to nonvanishing tensor components of the second-order nonlinear optical susceptibility.[29] The PMA_2PbCl_4 crystal is a type of layered perovskite and has exhibited ferroelectricity and piezoelectricity,[22,25] indicating its noncentrosymmetric nature. We adopted the temperature-lowering method to grow PMA_2PbCl_4 crystals (see the Experimental Section). The as-grown crystals exhibit defined hexagonal shapes with lateral sizes greater than 1 cm (see Figure S1 in the Supporting Information). The purity of the phase was confirmed by powder X-ray diffraction (Figure S2, Supporting Information). Single crystal X-ray diffraction was conducted on the synthesized crystals as well (**Figure 1**). The crystal structure

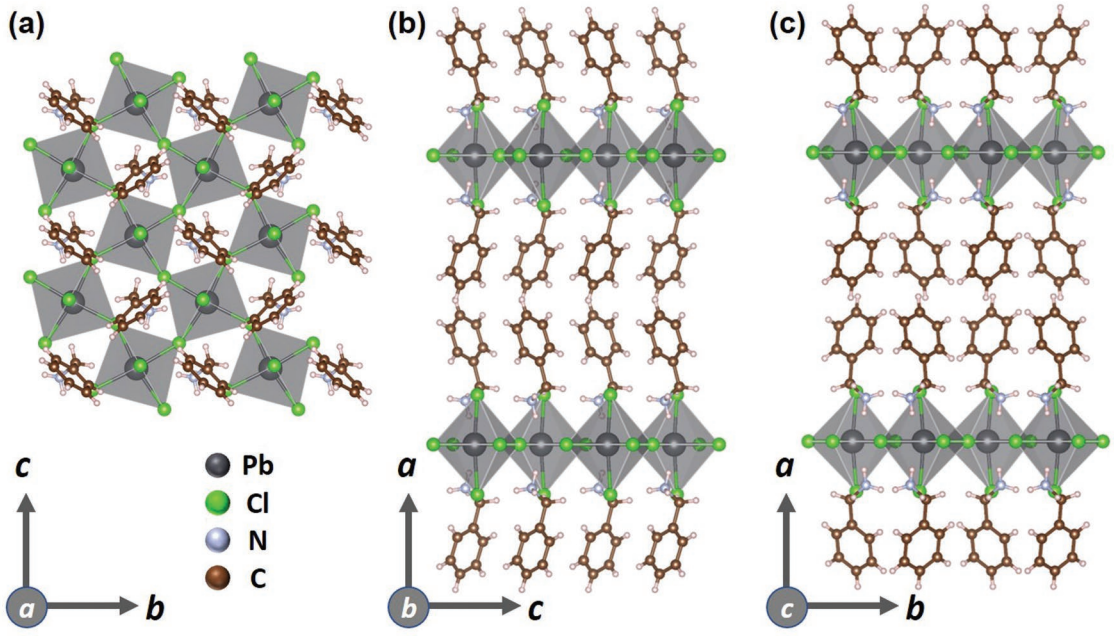

Figure 1. Crystal structure of PMA_2PbCl_4. The structure viewed along the a) *a*-axis, b) *b*-axis, and c) *c*-axis. A coherent off-centered shift of the Pb atoms and alignment of the PMA manifests along the *c*-axis.

displays a typical layered perovskite system, where an inorganic $PbCl_6$ network tethers PMA as the spacer cations.

As seen in Figure 1a, the lead atoms sit in the distorted octahedrons formed by the chloride ions with anisotropic Pb—Cl bonds. The layer formed by the corner sharing $PbCl_6$ octahedra extends throughout the crystallographic *bc*-plane. Viewed along the *b*-axis (Figure 1b), the Pb atoms (central coordinate: (0.5, 0.5, 0.41))—the centers of negative charge—display coherent off-centered displacement in the direction antiparallel to the *c*-axis. The layer spacing PMA cations and the C—N···Cl hydrogen bonds (central coordinate of N: (0.5, 0.5, 0.33)) exist with a collective tilting along the *c*-axis. Since there is a separation between the centers of positive and negative charge, an electric dipole moment forms in the unit cells and the addition of these dipoles (aligned along the *c*-axis) gives rise to overall spontaneous polarization in the crystal.[30] In contrast, as shown in Figure 1c, opposing dipole moments along the *a*- or *b*-axes cancel out the global polarization in these directions.

Angle-resolved Raman spectroscopy was performed to characterize the in-plane anisotropy of PMA_2PbCl_4 crystals. It has been demonstrated to be effective in observing optical and structural anisotropy in various 2D crystal systems.[31–33] In the back-scattering Raman and polarized detection configuration used here, the incident laser was along the *a*-axis of the crystal, and its initial polarization direction was set to coincide with the *c*-axis of the crystal (Figure S3a, Supporting Information). By sweeping the angle (θ) between laser polarization direction and crystal *c*-axis from 0° to 360°, a polar Raman plot of A_1 symmetric stretching of the [$PbCl_3$] pyramids[24] was obtained in **Figure 2**a. The strong anisotropic response indicates the optical anisotropy in the PMA_2PbCl_4 crystal (Note 1, Supporting Information).

The 2D nature of layered perovskites has prompted investigations of the out-of-plane birefringence.[34] In PMA_2PbCl_4 crystals, spontaneous polarization exists along the *c*-axis, and an additional in-plane anisotropy exists. This suggests that in-plane birefringence could also be observed from PMA_2PbCl_4 crystals. A circularly polarized laser beam was generated by using a quarter waveplate at 1550 nm. A sample of well-defined morphology was placed between two crossed polarizers. By simultaneously rotating these two crossed polarizers, we measured the transmitted optical power (Figure S4, Supporting Information). As can be seen from Figure 2b, there are four maxima and four minima. The transmitted power reaches a minimum when the first polarizer is parallel and perpendicular to the optical axis (0°, *c*-axis) and reaches a maximum when the first polarizer is 45° with respect to the optical axis. The birefringence measurement, in turn, confirms the anisotropy in the crystal. Variation of such birefringence with the electric field will be discussed in the latter part of this paper.

The imaginary part of the refractive index (κ) was determined by ellipsometry. κ, if it is positive, is the extinction coefficient, which characterizes the optical absorption of light in the material. The PMA_2PbCl_4 crystal is a direct-bandgap semiconductor[22] with a band gap of 3.65 eV (Figure S5, Supporting Information). The absorption is extremely low in the PMA_2PbCl_4 crystals beyond their first excitonic peak (329 nm) (Note 2, Supporting information), and hence they are suitable for polarizing devices that are designed to function across the visible and near-infrared spectra.

Powder second harmonic generation was obtained to verify the second-order optical nonlinearity of PMA_2PbCl_4 crystals (see Figure S6 in the Supporting Information).[35] The crystals were ground into powders with an average size of 100 μm. The powders were photoexcited using a 965 nm laser. Signals were collected after a 900 nm short-pass filter, and a sharp SHG peak was seen at 483 nm. The SHG from the PMA_2PbCl_4 crystals attests to their noncentrosymmetric structure and second-order optical nonlinearity. SHG is mainly due to the polarized electrons in the material. However, the linear EO effect originates from contributions from both electronic and ionic parts.[36] Therefore, the linear EO effect needs to be explored separately to gain a picture of the second-order optical nonlinearity of the material.

The linear EO effect (Pockels effect) offers a direct route to modify birefringence in the perovskite crystal. The linear EO coefficient was determined quantitatively at 1550 nm, the typical optical communications wavelength, where optical scattering and OH ion absorption is minimized.[37] **Figure 3**a shows a schematic of the measurement setup used to characterize the change of the in-plane birefringence caused by the linear EO effect:[5,38] a linearly polarized laser beam was launched normally to the surface of the sample and passed through two parallel electrodes, having a separation of 50 μm, touching the

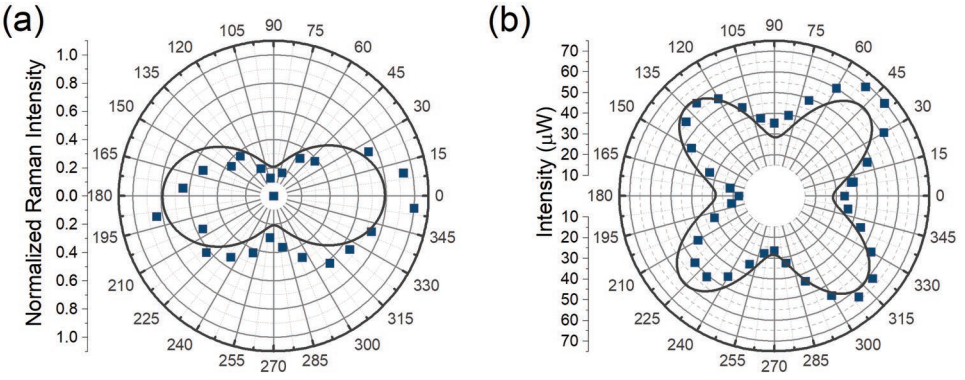

Figure 2. a) Normalized intensity of Raman mode 191.5 cm^{-1} with different excitation polarizations. b) Birefringence of the PMA_2PbCl_4 crystal. The transmitted power is measured by simultaneously rotating two crossed polarizers that sandwich the perovskite crystal. The data points are fitted with a $\sin^2$ function.

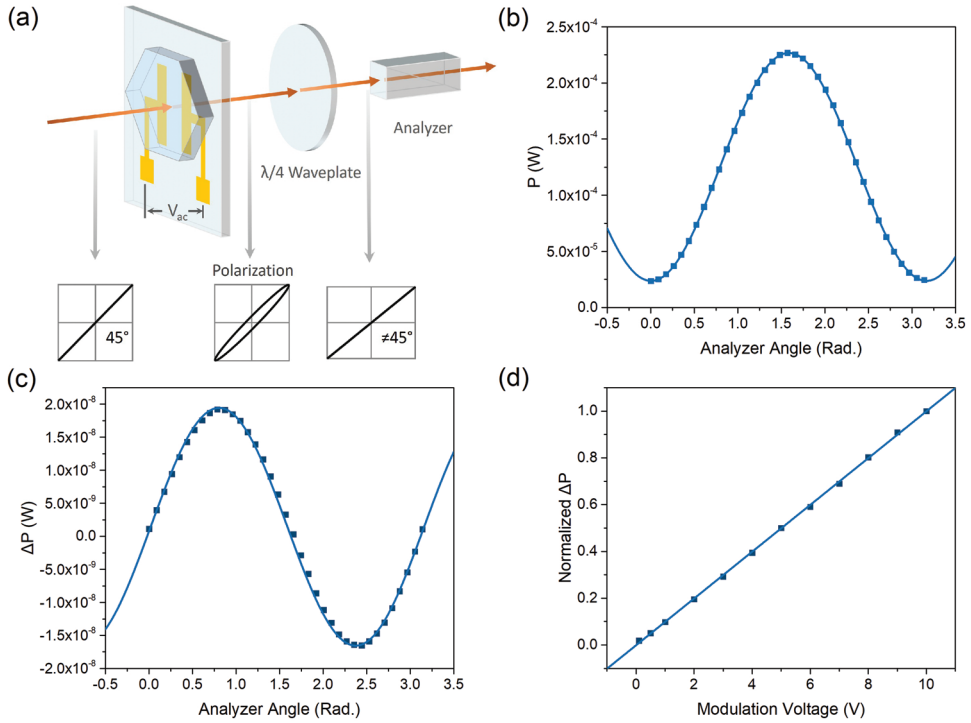

Figure 3. Electro-optic effect characterization. a) Schematics of the experimental setup used to determine the shift of the in-plane birefringence induced by the EO effect. 1550 nm laser beam with a polarization angle of 45° is launched on the sample. A modulation AC voltage V_{ac} is applied on the surface of the crystal with a pair of electrodes. The transmitted laser beam becomes elliptically polarized. It then passes through a 1550 nm quarter waveplate, and finally, the resulting linearly polarized light is analyzed with a Glan–Taylor polarizer. b) The variation of transmitted optical power (P) as a function of the polarization analyzer angle. c) The modulation of the transmitted optical power (ΔP) due to the EO effect as a function of the polarization analyzer angle. d) The linear growth of ΔP increasing with the modulation AC voltage at an analyzer position of 45°.

PMA_2PbCl_4 crystal. An electric field was applied parallel to the crystal surface along the c-axis and perpendicular to the incident light. The following expression was used to evaluate the shift in the electric field induced birefringence (see Note 3 in the Supporting Information)

$$\Delta n = \frac{1}{2} r_c n^3 E \tag{1}$$

The polarization of the incident beam was rotated by an angle of 45° with respect to the applied electric field. In order to characterize accurately the birefringence resulting from the applied electric field, we applied an AC voltage with a sinusoidal waveform and analyzed the optical signal using a lock-in amplifier. The frequency of the modulation voltage used was 6 kHz, and the peak-to-peak voltage was 10 V, which generated an electric field much smaller than the coercive force of the PMA_2PbCl_4 crystal.[22] As the laser beam passed through the crystal, the linearly polarized light became elliptically polarized due to the birefringence of the sample. A quarter waveplate ($\lambda/4$ plate) was used to compensate the phase change and return the beam to linear polarization. The polarization was therefore changed by a small angle, δ.[5] Finally, before the signal was collected by a Ge near infrared photodetector, a Glan laser calcite polarizer was placed to analyze the polarization of the resultant beam. When we vary the polarization analyzer angle, θ_a, the modulation AC field induced a power variation, ΔP, that should be proportional to the derivative of the total transmitted power P (see Note 3 in the Supporting Information)

$$\Delta P = \delta \frac{dP}{d\theta_a} \tag{2}$$

Figure 3c presents the measured evolution of ΔP that can be fit with Equation (2). The magnitude of the modulated transmitted power ΔP increases linearly as a function of the applied AC voltage (Figure 3d). These observations confirm the EO effect from the PMA_2PbCl_4 crystal. The linear increase of ΔP with applied voltage rules out the Kerr effect, which would manifest a quadratic relation.

The change of the polarization angle δ can be determined by fitting ΔP as a function of analyzer angle θ_a. The AC field induced phase change Γ is equal to $2 \times \delta$ and the EO coefficient along the c-axis,[38] r_c, can be written as[39]

$$r_c = \frac{\Gamma \lambda}{\pi n^3 t E_{ac}} \tag{3}$$

where t is the effective thickness of the perovskite crystal, and E_{ac} is the electric field along the c-axis. Therefore, we quantify the linear EO coefficient along the c-axis to be 1.40 pm V^{-1}. While the linear EO coefficient is not high in comparison to that of conventional nonlinear crystals (Table S1, Supporting Information), it is hoped that future studies will be motivated

Table 1. Optical linear and nonlinear electronic susceptibilities. Obtained from DFPT calculations.

Optical dielectric constant, $\varepsilon_{ij}^{\infty}(\omega)$		Nonlinear LEO susceptibility, $\chi_{ijk}^{(2)}(-\omega;\omega,0)$ [pm V^{-1}]	
ε_{11}	2.989	$\chi_{113}^{(2)}$	0.21
ε_{22}	2.978	$\chi_{223}^{(2)}$	–0.05
ε_{33}	2.819	$\chi_{333}^{(2)}$	1.49

to increase further the linear EO coefficients of this class of materials. We tried to pole the PMA_2PbCl_4 crystal by applying a DC voltage (100 V) that is greater than its coercive force. No significant enhancement of the EO response was observed (Figure S7, Supporting Information). We conclude that the domain size of the parallelly aligned dipoles on the PMA_2PbCl_4 crystal is at least larger than the gap between the electrodes (50 μm).

To complement the experimental investigations of the EO effect, we used DFT calculations on the nonlinear optical response of the layered perovskite. Through calculations done under electric field perturbations, we determined the optical dielectric constant (**Table 1**). PMA_2PbCl_4 shows biaxial birefringence with a considerable difference in refractive index along the *c*-axis and so the direction of polarization. Along with these quantities, the second-order linear EO susceptibilities can are determined (**Table 2**). The electronic contributions to the electro-optic coefficients are then estimated by combining these calculated quantities (Table 2). The linear EO coefficient along the *c*-axis is then $r_{33} - r_{23} = -0.39$ pm V^{-1}. This indicates that since the measured coefficient is much larger, the EO response derives mainly from ionic contributions, likely relating to the separation of the centers of the positive and negative ions. Note, the quantities calculated from DFT do not account for dispersion and represent the zero-frequency limits.

In sum, the off-centering of the metal cation (Pb) in the layered hybrid metal halide perovskite PMA_2PbCl_4, a trait of many inorganic perovskite nonlinear optical crystals, leads to inherent polarization. We show the in-plane birefringence of the PMA_2PbCl_4 crystals and present, for the first time for a hybrid metal halide perovskite, the modulation of such birefringence through the linear EO effect. We determined the effective linear EO coefficient. We demonstrated that the 2D metal halide perovskite network can act as a scaffold to anchor and align aromatic spacer cations to manifest an anisotropic structure over a large scale and produce an overall polarization in the crystal. The ability to align bulky spacer cations gives a degree of freedom for engineering the nonlinear properties of the layered perovskite. The flexibility of these materials and their solution-processing offers the potential for noncentrosymmetric layered metal halide perovskites to herald in new and compelling opportunities of low-cost high-performance EO modulation in telecommunications and interconnections.

Table 2. Electronic contributions to the linear electro-optic coefficients. Obtained from DFPT calculations.

Electro-optic tensor element	pm V^{-1}
r_{13}^{el}	–0.046
r_{23}^{el}	0.012
r_{33}^{el}	–0.38
r_{42}^{el}	–0.013
r_{51}^{el}	–0.049

Experimental Section

Crystal Growth: Phenylmethylammonium chloride (PMACl) was prepared by dissolving phenylmethylammonium in methanol and drop wise adding HCl solution (37%). The reaction was carried out in a flask in an ice bath, and the solution was stirred vigorously. The resultant white precipitation was washed with diethyl ether and methanol three times and dried in vacuum. The large PMA_2PbCl_4 crystal was prepared by adopting the temperature lowering method. PMACl (431 mg), $PbCl_2$ (417 mg), and 15 mL HCl aqueous solution (37%) were mixed in a 20 mL vial. The mixture was fully dissolved after it was heated to 100 °C. After that, the temperature was decreased at a rate of 20 °C per day. Large transparent crystals were obtained at the end.

X-Ray Crystallographic Analysis: A small fraction of the crystal was cleaved from the as-grown PMA_2PbCl_4 crystal. Single crystal X-ray diffraction data were collected at room temperature on a Bruker Kappa APEX-DUO diffractometer equipped with a rotating anode with graphite-monochromated Mo-Kα radiation (Burker Triumph, λ = 0.71073Å). Both φ scans and ω scans were conducted. SADABS was adopted for absorption corrections.[40] Fitting and refinement (full-matrix least-squares refinement based on F^2) of single-crystal structures were performed with SHELXT and SHELXL-2016/6, respectively.[41a,b] All the hydrogen atoms were included in the position calculation, which allowed the refinement with the riding-motion approximation.

Angle-Resolved Raman Spectroscopy: Raman spectra were recorded on a home-made Raman spectrometer with a 532 nm excitation laser in the backscattering configuration with a 1200 mm^{-1} grating and Andor 750 spectrometer. The spot size of the focused laser was ≈1 μm, and the laser power was 47 μW. Angle-resolved Raman spectra were recorded in the condition that the incident light and the scattered light were aligned parallel to each other. The angle θ was defined as the angle between the *c*-axis and excitation laser polarization and was swept from 0° to 360° with a 15° step size by rotating a half-wave plate.

Density Functional Theory: DFT calculations were implemented using the Quantum Espresso software.[42] Norm-conserving pseudopotentials produced with the Troullier–Martins method were used.[43] Calculations were done within the local density approximation using Perdew–Wang exchange-correlation functionals.[44] Lattice constants were kept at the values obtained from single crystal X-ray diffraction, while atomic positions were relaxed so that internal forces were less than 1×10^{-4} Ry Bohr^{-1}. An energy cut-off of 60 Ry and Monkhorst–Pack *k*-point grid of $6 \times 6 \times 6$ was used. Density functional perturbation theory calculations were done to determine the linear and nonlinear electronic susceptibilities.[45] The nonlinear susceptibilities were determined within the $2n + 1$ theorem.

Supporting Information

Supporting Information is available from the Wiley Online Library or from the author.

Acknowledgements

Y.G. and G.W. contributed equally to this work. This work was financially supported by Natural Sciences and Engineering Research Council (NSERC). G.W. acknowledges funding from NSERC. M.I.S. acknowledges the support of Banting Postdoctoral Fellowship Program.

Conflict of Interest

The authors declare no conflict of interest.

Keywords

2D material, birefringence, electro-optic modulation, metal halide perovskite, nonlinear optics

Received: December 27, 2018
Revised: February 7, 2019
Published online:

[1] G. T. Reed, G. Mashanovich, F. Y. Gardes, D. J. Thomson, *Nat. Photonics* **2010**, *4*, 518.
[2] S. Ken-ichi, M. Yasunori, A. Hiroyuki, N. Eiji, K. Mikihiko, H. Tomoyuki, I. Daisuke, K. Akihiro, H. Ken-ichi, I. Takuro, *Jpn. J. Appl. Phys.* **1995**, *34*, 5443.
[3] M. G. Harwood, P. Popper, D. F. Rushman, *Nature* **1947**, *160*, 58.
[4] L. Chen, R. M. Reano, *Opt. Express* **2012**, *20*, 4032.
[5] S. Abel, T. Stöferle, C. Marchiori, C. Rossel, M. D. Rossell, R. Erni, D. Caimi, M. Sousa, A. Chelnokov, B. J. Offrein, J. Fompeyrine, *Nat. Commun.* **2013**, *4*, 1671.
[6] P. Dong, S. Liao, D. Feng, H. Liang, D. Zheng, R. Shafiiha, C.-C. Kung, W. Qian, G. Li, X. Zheng, A. V. Krishnamoorthy, M. Asghari, *Opt. Express* **2009**, *17*, 22484.
[7] J.-M. Brosi, C. Koos, L. C. Andreani, M. Waldow, J. Leuthold, W. Freude, *Opt. Express* **2008**, *16*, 4177.
[8] J. Leuthold, C. Koos, W. Freude, *Nat. Photonics* **2010**, *4*, 535.
[9] S. R. Marder, B. Kippelen, A. K. Y. Jen, N. Peyghambarian, *Nature* **1997**, *388*, 845.
[10] S. Koeber, R. Palmer, M. Lauermann, W. Heni, D. L. Elder, D. Korn, M. Woessner, L. Alloatti, S. Koenig, P. C. Schindler, H. Yu, W. Bogaerts, L. R. Dalton, W. Freude, J. Leuthold, C. Koos, *Light: Sci. Appl.* **2015**, *4*, e255.
[11] N. Cho, F. Li, B. Turedi, L. Sinatra, S. P. Sarmah, M. R. Parida, M. I. Saidaminov, B. Murali, V. M. Burlakov, A. Goriely, O. F. Mohammed, T. Wu, O. M. Bakr, *Nat. Commun.* **2016**, *7*, 13407.
[12] D. N. Dirin, I. Cherniukh, S. Yakunin, Y. Shynkarenko, M. V. Kovalenko, *Chem. Mater.* **2016**, *28*, 8470.
[13] S. Hu, H. Gao, Y. Qi, Y. Tao, Y. Li, J. R. Reimers, M. Bokdam, C. Franchini, D. Di Sante, A. Stroppa, W. Ren, *J. Phys. Chem. C* **2017**, *121*, 23045.
[14] Z. Fan, J. Xiao, K. Sun, L. Chen, Y. Hu, J. Ouyang, K. P. Ong, K. Zeng, J. Wang, *J. Phys. Chem. Lett.* **2015**, *6*, 1155.
[15] S. T. Birkhold, H. Hu, P. T. Höger, K. K. Wong, P. Rieder, A. Baumann, L. Schmidt-Mende, *J. Phys. Chem. C* **2018**, *122*, 12140.
[16] S. G, P. Mahale, B. P. Kore, S. Mukherjee, M. S. Pavan, C. De, S. Ghara, A. Sundaresan, A. Pandey, T. N. Guru Row, D. D. Sarma, *J. Phys. Chem. Lett.* **2016**, *7*, 2412.
[17] R. Zhang, J. Fan, X. Zhang, H. Yu, H. Zhang, Y. Mai, T. Xu, J. Wang, H. J. Snaith, *ACS Photonics* **2016**, *3*, 371.
[18] L. Wu, K. Chen, W. Huang, Z. Lin, J. Zhao, X. Jiang, Y. Ge, F. Zhang, Q. Xiao, Z. Guo, Y. Xiang, J. Li, Q. Bao, H. Zhang, *Adv. Opt. Mater.* **2018**, *6*, 1800400.
[19] G. Walters, B. R. Sutherland, S. Hoogland, D. Shi, R. Comin, D. P. Sellan, O. M. Bakr, E. H. Sargent, *ACS Nano* **2015**, *9*, 9340.
[20] X. Q. Liu, J. W. Wu, X. X. Shi, H. J. Zhao, H. Y. Zhou, R. H. Qiu, W. Q. Zhang, X. M. Chen, *Appl. Phys. Lett.* **2015**, *106*, 202903.
[21] S. Yoshida, H. Akamatsu, R. Tsuji, O. Hernandez, H. Padmanabhan, A. Sen Gupta, A. S. Gibbs, K. Mibu, S. Murai, J. M. Rondinelli, V. Gopalan, K. Tanaka, K. Fujita, *J. Am. Chem. Soc.* **2018**, *140*, 15690.
[22] W.-Q. Liao, Y. Zhang, C.-L. Hu, J.-G. Mao, H.-Y. Ye, P.-F. Li, S. D. Huang, R.-G. Xiong, *Nat. Commun.* **2015**, *6*, 7338.
[23] H.-Y. Ye, Y.-Y. Tang, P.-F. Li, W.-Q. Liao, J.-X. Gao, X.-N. Hua, H. Cai, P.-P. Shi, Y.-M. You, R.-G. Xiong, *Science* **2018**, *361*, 151.
[24] C. C. Stoumpos, L. Frazer, D. J. Clark, Y. S. Kim, S. H. Rhim, A. J. Freeman, J. B. Ketterson, J. I. Jang, M. G. Kanatzidis, *J. Am. Chem. Soc.* **2015**, *137*, 6804.
[25] K.-z. Du, Q. Tu, X. Zhang, Q. Han, J. Liu, S. Zauscher, D. B. Mitzi, *Inorg. Chem.* **2017**, *56*, 9291.
[26] H.-Y. Ye, W.-Q. Liao, C.-L. Hu, Y. Zhang, Y.-M. You, J.-G. Mao, P.-F. Li, R.-G. Xiong, *Adv. Mater.* **2016**, *28*, 2579.
[27] Z. Sun, X. Liu, T. Khan, C. Ji, M. A. Asghar, S. Zhao, L. Li, M. Hong, J. Luo, *Angew. Chem., Int. Ed.* **2016**, *55*, 6545.
[28] K.-T. Ho, S.-F. Leung, T.-Y. Li, P. Maity, B. Cheng, H.-C. Fu, O. F. Mohammed, J.-H. He, *Adv. Mater.* **2018***30*, 1804372.
[29] A. Yariv, P. Yeh, *Photonics: Optical Electronics in Modern Communications*, Oxford, **2007**, p. 356.
[30] M. Dawber, *Physics* **2012**, *5*, 63.
[31] H. Yang, H. Jussila, A. Autere, H.-P. Komsa, G. Ye, X. Chen, T. Hasan, Z. Sun, *ACS Photonics* **2017**, *4*, 3023.
[32] S. Niu, G. Joe, H. Zhao, Y. Zhou, T. Orvis, H. Huyan, J. Salman, K. Mahalingam, B. Urwin, J. Wu, Y. Liu, T. E. Tiwald, S. B. Cronin, B. M. Howe, M. Mecklenburg, R. Haiges, D. J. Singh, H. Wang, M. A. Kats, J. Ravichandran, *Nat. Photonics* **2018**, *12*, 392.
[33] H. B. Ribeiro, M. A. Pimenta, C. J. S. de Matos, R. L. Moreira, A. S. Rodin, J. D. Zapata, E. A. T. de Souza, A. H. Castro Neto, *ACS Nano* **2015**, *9*, 4270.
[34] A. Fieramosca, L. De Marco, M. Passoni, L. Polimeno, A. Rizzo, B. L. T. Rosa, G. Cruciani, L. Dominici, M. De Giorgi, G. Gigli, L. C. Andreani, D. Gerace, D. Ballarini, D. Sanvitto, *ACS Photonics* **2018**, *5*, 4179.
[35] S. K. Kurtz, T. T. Perry, *J. Appl. Phys.* **1968**, *39*, 3798.
[36] F. Wang, *Phys. Rev. B* **1999**, *59*, 9733.
[37] J. C. Daly, *Fiber Optics*, Taylor & Francis, Boca Raton, Florida, USA **1984**, p. 165.
[38] H. Adachi, T. Kawaguchi, K. Setsune, K. Ohji, K. Wasa, *Appl. Phys. Lett.* **1983**, *42*, 867.
[39] D. H. Reitze, E. Haton, R. Ramesh, S. Etemad, D. E. Leaird, T. Sands, Z. Karim, A. R. Tanguay Jr., *Appl. Phys. Lett.* **1993**, *63*, 596.
[40] Bruker, *APEX2, SAINT & SADABS Bruker AXS Inc.*, Madison, Wisconsin, USA **2007**.
[41] a) G. Sheldrick, *Acta Crystallogr. A* **2015**, *71*, 3; b) G. Sheldrick, *Acta Crystallogr. C* **2015**, *71*, 3.
[42] P. Giannozzi, S. Baroni, N. Bonini, M. Calandra, R. Car, C. Cavazzoni, D. Ceresoli, G. L. Chiarotti, M. Cococcioni, I. Dabo, *J. Phys.: Condens. Matter* **2009**, *21*, 395502.
[43] N. Troullier, J. L. Martins, *Phys. Rev. B* **1991**, *43*, 1993.
[44] J. P. Perdew, Y. Wang, *Phys. Rev. B* **1992**, *45*, 13244.
[45] S. Baroni, S. de Gironcoli, A. Dal Corso, P. Giannozzi, *Rev. Mod. Phys.* **2001**, *73*, 515.